Contrib Mineral Petrol (2016) 171:29
DOI 10.1007/s00410-016-1243-y

ORIGINAL PAPER

Highly siderophile element abundances in Eoarchean komatiite and basalt protoliths

Elizabeth A. Frank[1,4] · Wolfgang D. Maier[2] · Stephen J. Mojzsis[1,3]

Received: 11 September 2015 / Accepted: 17 February 2016 / Published online: 12 March 2016

Abstract Plume-derived, Mg-rich, volcanic rocks (komatiites, high-Mg basalts, and their metamorphic equivalents) can record secular changes in the highly siderophile element (HSE) abundances of mantle sources. An apparent secular time-dependent enrichment trend in HSE abundances from Paleoarchean to Paleoproterozoic mantle-derived rocks could represent the protracted homogenization of a Late Veneer chondritic contaminant into the pre-Late Veneer komatiite source. To search for a possible time dependence of a late accretion signature in the Eoarchean mantle, we report new data from rare >3700 Myr-old mafic and ultramafic schists locked in supracrustal belts from the Inukjuak domain (Québec, Canada) and the Akilia association (West Greenland). Our analysis shows that some of these experienced HSE mobility and/or include a cumulate component (Touboul et al. in Chem Geol 383:63–75, 2014), whereas several of the oldest samples show some of the most depleted HSE abundances measured for rocks of this composition. We consider these new data for the oldest documented rocks of komatiite protolith in light of the Late Veneer hypothesis.

Keywords Late Veneer · Komatiites · Highly siderophile elements · Platinum group elements · Mantle evolution · Eoarchean

Communicated by Hans Keppler.

Stephen J. Mojzsis: Collaborative for Research in Origins (CRiO).

Electronic supplementary material The online version of this article (doi:10.1007/s00410-016-1243-y) contains supplementary material, which is available to authorized users.

✉ Elizabeth A. Frank
efrank@carnegiescience.edu

✉ Stephen J. Mojzsis
mojzsis@colorado.edu

[1] Department of Geological Sciences, NASA Lunar Science Institute, Center for Lunar Origin and Evolution (CLOE), University of Colorado, 2200 Colorado Avenue, UCB 399, Boulder, CO 80309-0399, USA

[2] School of Earth and Ocean Sciences, Cardiff University, Main Building, Park Place, Cardiff CF10 3AR, UK

[3] Institute for Geological and Geochemical Research, Hungarian Academy of Sciences, Budaörsi ut 45, Budapest 1112, Hungary

[4] Present Address: Department of Terrestrial Magnetism, Carnegie Institution of Washington, 5241 Broad Branch Road NW, Washington, DC 20015-1305, USA

Introduction

During the primary accretion phase of early solar system bombardment, as metallic cores grew within large differentiated planetary embryos, the highly siderophile elements (HSE) should have been effectively stripped from silicate mantles via strong metal–silicate partitioning of the HSE component into metal phases; these were then segregated into metallic cores (e.g., Stevenson 1981). Metal–silicate partition coefficients ($D^{met/sil}$) of the HSE, which include the platinum group elements (PGE: Os, Ir, Ru, Rh, Pt, and Pd), Au, and Re, are mainly constrained through experiments performed at ~1 bar, with all having $D^{met/sil}$ values $>10^3$ (e.g., Mann et al. 2012 and references therein). While it is well established that the HSE partition very strongly from silicate into metal, it has also been shown that the different elements in this class do not have identical D values under the same conditions of high temperature and pressure that were present at the base of Earth's early magma ocean.

Specifically, the iridium-series subgroup (IPGE; Ir, Ru, and Os) behaves highly compatibly relative to the platinum-series subgroup (PPGE; Pt, Pd, and Rh), which, along with Re and Au, is moderately compatible to moderately incompatible (Barnes et al. 1985). The elements in the IPGE and PPGE subgroups should have each behaved differently in the melts that formed at the time of core formation and separation of the silicate reservoirs. Hence, the different subgroups of HSE are expected to show different degrees of fractionation relative to chondrites and as a result, variable relative concentrations in Earth's mantle. It has long been known, however, that this is not the case for terrestrial rocks. Instead, the HSE are present in modern mafic and ultramafic extrusive igneous rocks at concentrations several orders of magnitude higher than those predicted based on simple partitioning behavior (Kimura et al. 1974).

Komatiites are volcanic rocks of peridotitic composition with >18 wt% MgO that can be used as archives of Archean mantle chemical evolution (Arndt et al. 2008). Such rocks are strongly enriched in the HSE compared to many kinds of mafic crustal rocks and much more so than any normal felsic suite. Sourced from mid- to deep-mantle reservoirs, komatiites are generally regarded to have formed at relatively high degrees of partial melting (20–50 %; Arndt 2003) as a result of the elevated temperatures of the young mantle (e.g., Richter 1988; Grove et al. 1999; Herzberg et al. 2010). This is supported by the broad (but not temporally exclusive; cf. Echeverría 1980; Hanski et al. 2004) restriction of komatiites to Archean and Early Proterozoic terranes. Analyses of Pt and Ru in Archean ultramafic volcanic rocks (komatiite *s.s.*) as old as about 3.5 Ga seem to show a secular HSE depletion in the mid- to deep-mantle reservoirs from which such rocks are sourced (Maier et al. 2009). It is surprising that the mantle should contain so much as ppb-level abundances of the HSE given that, as described above, core formation should have effectively stripped these elements from the silicate Earth.

Even more surprising is the observation that the HSE are present in approximately chondritic relative abundances in Earth's mantle despite displaying different metal-silicate partitioning behaviors between the elements. One explanation for this phenomenon is that a late accretion event (dubbed the "Late Veneer") supplemented the mantle with primitive CI-chondrite material (Chou 1978). Late accretion was "late" in the sense that it must have occurred after core formation and, consequently, the chemical separation of the core from the mantle (Fig. 1). It is widely accepted that the last time this happened was at the Moon-forming event approximately 4.5 Gyr ago (e.g., Wood and Halliday 2005; Halliday 2008). If it is assumed that the delivered material that polluted the mantle with metals after core closure was of chondritic composition, approximately ~0.5–1 % of Earth's mantle mass is required to cause the

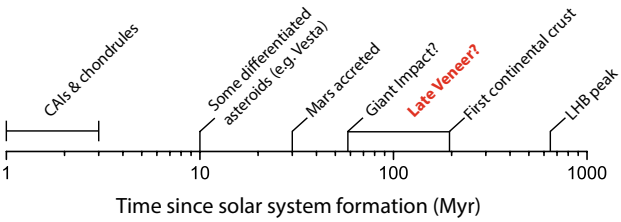

Fig. 1 Timeline showing early solar system events and probable timing of the Late Veneer

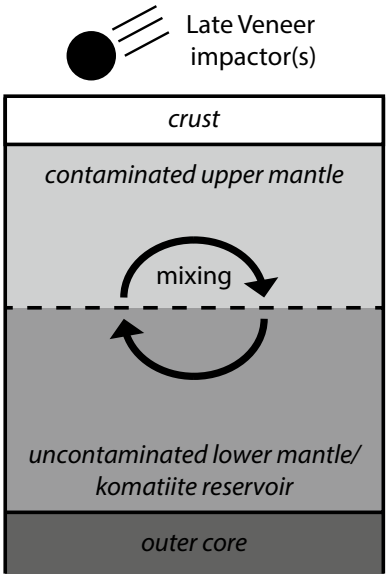

Fig. 2 Schematic of the Late Veneer scenario as proposed by Maier et al. (2009) and dubbed "trickle-down geodynamics" by Arndt (2009)

observed HSE signatures (Chou 1978; Walker 2009). A single chondritic impactor of that size corresponds to a differentiated body approximately 2700 km in diameter (Bottke et al. 2010). Based on current understanding, the presence of objects this large at the time of the Late Veneer (hereafter, LV) can be explained by a leftover population from planetary accretion (e.g., Walsh et al. 2011), but a multiple impactor scenario of later oxidized bodies cannot be ruled (Rubie et al. 2011). It is important to emphasize that the LV should not be conflated with the so-called Late Heavy Bombardment, which minimally affected Earth's composition (Abramov and Mojzsis 2009). We return to this point later.

The LV scenario was favored by Maier et al. (2009) to explain the depleted HSE abundances in Archean komatiites, but this mechanism is only viable if the delivered material penetrated no farther than the upper mantle far away

from the deep komatiite source (Dahl and Stevenson 2010). It is unclear how a signal from late accretion by the mechanisms cited above could become suspended in a relatively small volume in the uppermost mantle. Simulations of the impact of a lunar mass object with Earth to explore the physical and chemical consequences of a 0.5–1 wt% Late Veneer addition have yet to be published. Within this framework of our present state of knowledge, Arndt (2009) coined the term "trickle-down geodynamics" to describe an early scenario in which the Hadean deep mantle was relatively depleted in HSE until the uppermost mantle regions, refertilized by HSE-rich components, were mixed throughout (Fig. 2). The secular rise in mantle source Pt and Ru concentrations appears to have started at about 3 Ga as reported in Maier et al. (2009), but that earlier data set only extended to samples no older than ca. 3.5 Ga. An exogenous explanation for the CI-relative abundances of the HSE involving a Late Veneer is not universally accepted, however, and the subject of these elements in the mantle has sparked vigorous debate with alternative scenarios (Willbold et al. 2011; Touboul et al. 2012; Puchtel et al. 2014; Touboul et al. 2014; Willbold et al. 2015; cf. Righter et al. 2015).

More komatiite analyses from older rocks are required to settle the debate, but the global sample selection of Eoarchean extrusive ultramafic rocks is severely limited. Rocks of komatiitic affinity have previously been inferred from rare ultramafic schists documented in ancient gneiss complexes that are at least 3.7 Ga in age (Nutman et al. 1996; Anbar et al. 2001). Published data for samples of probable komatiite protoliths older than about 3.5 Ga that can be used to further explore the trend noted by Maier et al. (2009) are sparse, especially for major and trace element compositions (Touboul et al. 2014; Rizo et al. 2016). To overcome these limitations, we analyzed well-characterized Eoarchean schists interpreted from field associations, mineralogy, and bulk chemistry to represent komatiite and komatiitic basalt protoliths from Eoarchean supracrustal enclaves. These were collected by us in the ca. 3.77–3.83 Ga Akilia association (Itsaq Gneiss Complex) in southern West Greenland (Manning et al. 2006; Cates and Mojzsis 2006), and the ca. 3.78 Ga (possibly ca. 4.38 Ga; O'Neil et al. 2012) ultramafic rocks from the Porpoise Cove locality, Nuvvuagittuq supracrustal belt of the Inukjuak domain in northern Québec (Cates and Mojzsis 2007; Cates et al. 2013). Since the available rock suite from Eoarchean terranes is so limited, we also chose to analyze eight amphibolites (so-called meta-basalts) from the Porpoise Coves outcrops in the Nuvvuagittuq area, even though we demonstrate that these samples are not of sufficient quality for our purposes. We use these new ultramafic HSE data to further explore the hypothesis that observed trends could have arisen from a mixing-in of a postulated Late Veneer component. The time required for the dynamic chemical homogenization of an HSE contaminant is consistent with proposed Hadean (slow) mantle stirring rates (O'Neill et al. 2013), protracted (early) crustal recycling times (~750 Myr) as derived from coupled $^{146,147}Sm/^{143,142}Nd$ systematics (e.g., Roth et al. 2014), and the progressive mixing-in of a low $^{182}W/^{184}W$ chondritic-type tungsten component from a postulated LV contaminant (e.g., Willbold et al. 2011, 2015).

Samples and analytical techniques

Eoarchean ultramafic samples

The samples investigated herein derive from our detailed field sampling in the Nuvvuagittuq supracrustal belt (ca. 3.78 Ga; Cates et al. 2013) in northern Québec (Canada) and the Akilia association (McGregor and Mason 1977). The latter include rocks of the type locality on Akilia (island) and the Innersuartuut outcrops described in Cates and Mojzsis (2006) that are part of the 3.77–3.83 Ga Færinghavn terrane, Itsaq Gneiss Complex in southern West Greenland (Nutman et al. 1996). As detailed in McGregor and Mason (1977) and McLennan et al. (1984), the Akilia association is comprised of interleaved m- to km-scale enclaves of mafic, ultramafic, and Fe-rich paragneisses of sedimentary derivation within variably deformed Eoarchean granitoid (previously termed "Amîtsoq") gneisses. The Nuvvuagittuq supracrustals are dominantly composed of large (~1–5 km^2) strongly deformed amphibolitic + paragneissic enclaves surrounded and in some cases intruded by granitoid gneisses of the Eoarchean–Paleoarchean Voizel suite. Full descriptions of whole-rock analyses for the samples reported here and details of their geological settings and context can be found in (Manning et al. 2006; Cates and Mojzsis 2006; Dauphas et al. 2007; Cates and Mojzsis 2007; 2009; Cates et al. 2013). Whole-rock major, minor, and trace element geochemistry for our high-magnesium samples from Akilia (*GR9703*, *GR97M22*, *GR0019*, *GR0020*, *GR0030*, and *GR0031*), Innersuartuut (*GR04064* and *GR04065*), and Nuvvuagittuq (*IN05047* and *IN08016*) are reported in Table 1.

At every stage in this project, care was taken to select samples that are unassociated with sulfide deposits. High eruption temperatures (~1650 °C; Green 1975) at time of emplacement means that some komatiites could have assimilated sulfur from crustal rocks. If this happens, it is possible that an immiscible sulfide melt exsolved that extracted the HSE—and thus, any Late Veneer signature—from the magmas (Lesher and Keays 2002). In their analysis, Maier et al. (2009) reported HSE data only from komatiites not known to be associated with sulfide deposits or sulfide mineralization, and we follow the same guidelines herein.

Table 1 Whole-rock geochemistry for the ultramafic samples

Sample	GR9703	GR0019	GR0020	GR0030	GR0031	GR97M22	GR04064	GR04065	IN05047	IN08016
Locality	Akilia Island	Akilia Island	Akilia Island	Akilia Island	Akilia Island	Innersuar-tuut	Innersuar-tuut	Innersuar-tuut	Nuvvuagit-tuq	Nuvvuagit-tuq
Age (Ma)	3825	3825	3825	3825	3825	3750	3750	3750	3740	3750
Reference	1	2	2	2	2	3	4	4	5, 6	7
SiO_2	48.67	46.73	46.52	45.84	47.17	45.00	39.99	50.42	42.40	49.06
TiO_2	0.3	0.38	0.28	0.46	0.34	0.32	0.13	0.20	0.894	0.374
Al_2O_3	8.19	8.58	8.5	10.25	7.77	3.08	4.57	5.28	6.40	5.19
MgO	22.29	21.03	25.3	13.8	23.28	26.82	35.69	18.43	22.56	17.17
Fe_2O_3	10.87	12.43	10.90	12.86	11.64	12.26	11.66	9.52	20.04	14.64
MnO	0.18	0.18	0.16	0.18	0.16	0.25	0.18	0.20	0.22	0.26
CaO	4.18	6.39	4.79	12.44	5.2	9.31	2.12	12.79	1.03	10.58
Na_2O	0.98	1.13	0.82	1.19	0.84	0.31	0.17	1.10	0.07	0.43
K_2O	1.97	0.15	0.08	0.43	0.1	0.22	0.91	0.26	0.03	0.07
P_2O_5	0.02	0.02	0.02	0.3	0.02	0.04	0.01	0.03	0.08	0.11
LOI	1.95	2.44	2.35	1.45	3.17		4.08	1.62	5.47	2.77
Total	99.59	98.23	98.64	97.66	98.49	97.61	99.52	99.85	99.2	100.7
Rb		3	2	16	0		106	12.5	0.44	0.332
Sr		13	19	33	11		3.82	23.9	1.21	1.815
Ba		5	4	12	4		10.1	15.7	1.3	<D.L.
Sc		35	38	40	31		16.3	15.2		
Nb							0.29	1.65	2.82	1.107
Ta							0.54	0.56	0.2	0.33
Y		9	7	12	8		2.69	7.22	9.57	21.87
Zr	26	26	23	33	22		2.61	8.77	34.4	24.46
Ni	729	725	971	323	1150	1580	1884	640	977.4	855.8
Cr	2367	3180	2300	1570	2720	5540	2451	1504	3098	1680
V							58.3	104	196	113.1
Co	79	73	83	68	87					181.7
Cu							4.80	69.3	147	350
Zn							92.0	121	121	54
La		2.80	1.30	2.50	1.80		0.42	2.05	2.17	2.248
Ce		5.20	2.60	5.00	3.80		1.08	6.93	6.23	5.409
Pr		0.65	0.35	0.70	0.48		0.15	1.19	1.04	0.839
Nd		3.60	2.20	4.30	3.00		0.59	6.41	5.59	4.455
Sm		1.10	0.70	1.30	0.90		0.21	1.83	1.63	1.75
Eu		0.52	0.25	0.42	0.34		0.10	0.36	0.26	0.57
Gd		1.40	1.00	1.60	1.20		0.35	1.82	1.88	2.821
Tb		0.30	0.20	0.30	0.20		0.07	0.26	0.31	0.533
Dy		1.80	1.30	2.20	1.50		0.41	1.37	1.98	3.562
Ho		0.40	0.30	0.50	0.30		0.11	0.28	0.39	0.751
Er		1.20	1.00	1.40	1.00		0.31	0.76	1.13	2.088
Tm		0.18	0.15	0.22	0.15		0.05	0.12	0.159	0.312
Yb		1.20	1.00	1.50	1.00		0.30	0.79	1.03	2.017
Lu		0.18	0.17	0.22	0.16		0.05	0.12	0.159	0.3
Hf		0.9	0.6	1.1	0.8		0.11	0.30	1.0	0.69
Th		0.3	0.1	0.2	0.2		0.04	0.09	0.2	0.17
U		0.2		0.2	0.3		0.04	0.10	0.0	0.07
Pb	5						1.16	2.30	0.1	3.92

Data come from (1) this study, (2) Manning et al. (2006), (3) McGregor and Mason (1977), (4) Cates and Mojzsis (2006), (5) Cates and Mojzsis (2007), (6) Dauphas et al. (2007), and (7) Cates et al. (2013). Sample *GR97M22* is reported here but not included in analyses

Akilia association: GR9703, GR97M22, GR0019, GR0020, GR0030, GR0031

Sample *GR9703* is a "metakomatiite" from the main body of supracrustal rocks from the type locality of the Akilia association located on the southwest peninsula of Akilia island (Anbar et al. 2001); it closely corresponds to *GR0019* reported in Manning et al. (2006). Sample *GR97M22* was not analyzed for its major, minor, and trace element content but is identical to *131477* as reported in McGregor and Mason (1977; V. McGregor, *personal communication to S. Mojzsis, July 1997*). Sample *131477* showed high Cr (5540 ppm) and Ni (1580 ppm), and its overall composition was interpreted to be similar to that of Onverwacht Group komatiites (Viljoen and Viljoen 1969) and, except for Al_2O_3 and CaO, the average komatiite from Munro Township (Arndt et al. 1977). Although we report HSE measurements of *GR97M22*, we do not include them in our HSE trend analyses as explained later.

Samples *GR0019*, *GR0020*, *GR0030*, and *GR0031* all come from the same ultramafic locality at Akilia reported in Manning et al. (2006). They derive from ultramafic units that occur as irregular blocks to oblate lenses <1 m to several m in size within a larger mafic unit locked in a strongly deformed metamorphosed volcano-sedimentary (supracrustal) succession. Based on the MgO content (13.8 wt%) of the rock, sample *GR0030* may be classified as a basaltic komatiite and we group it with the ultramafic samples.

Innersuartuut: GR04064, GR04065

High-magnesium samples *GR04064* and *GR04065* have compositions intermediate between abyssal peridotite and basaltic komatiite, although their parentages are different (Cates and Mojzsis 2006). The samples were collected from a supracrustal enclave on Innersuartuut that preserves a mappable succession of metamorphosed volcanic and sedimentary rocks, including quartz–magnetite–pyroxene rocks, banded iron formations, and quartz–biotite schists.

Nuvvuagittuq: IN05047, IN08016

Both ultramafic samples from this collection show depleted Al relative to Ti. Sample *IN05047* is associated with nearby banded iron formations and preserves putative pillow structures. Cates and Mojzsis (2007) interpreted this rock to be derived from a melt originating from a source with garnet as a residual phase, consistent with Barberton-type komatiites (see also Dauphas et al. 2007). With 17.17 wt% MgO, *IN08016* is very close to the subjective 18 wt% MgO cutoff for a komatiite proposed by Arndt et al. (2008). It contains 855.8 ppm Ni and 1680 ppm Cr (Cates et al. 2013), consistent with komatiite-like abundances. Thus, we treat this rock as a probable komatiite.

Mafic samples from Nuvvuagittuq

All the mafic samples reported here were collected from the Nuvvuagittuq localities (Table 2). They include three hornblende amphibolites (*IN05013*, *IN05019*, *and IN05021)*, four cummingtonite-rich (Ca-poor) amphibolites (*IN08012*, *IN08017, IN08043*, *and IN08044*), and one plagioclase-rich amphibolite (*IN05046*). Sample *IN05013* is a plagioclase-rich hornblende amphibolite captured within a succession of banded iron formations at the Porpoise Cove outcrops (O'Neil et al. 2007). Samples *IN05019* and *IN05021* are massive hornblende amphibolites with low Al_2O_3/TiO_2 ratios (Dauphas et al. 2007; Cates and Mojzsis 2007). The Al_2O_3/TiO_2 ratios of samples from Nuvvuagittuq were used by O'Neil et al. (2007, 2011) to develop a classification scheme that bears some resemblance to the komatiite classification system cited above. Thus, medium and high Al_2O_3/TiO_2 and Ca-poor, cummingtonite-rich amphibolites are proposed to have crystallized from melts that formed in the presence of garnet (O'Neil et al. 2007, 2011; Cates et al. 2013). Sample *IN08017*, another cummingtonite-rich amphibolite, has a medium Al_2O_3/TiO_2 ratio, while *IN08012*, *IN08043*, and *IN08044* are all cummingtonite-rich amphibolites with low Al_2O_3/TiO_2 ratios, interpreted to have formed without residual garnet.

Analytical techniques

Whole-rock samples were crushed and powdered at the Department of Geological Sciences of the University of Colorado in agate mortars pre-cleaned with quartz sand and subsequently conditioned with small sample aliquots prior to powdering of the main sample mass of approximately 30 g. Care was taken in all steps, from sample acquisition to processing, to avoid contact with metal implements and to process enough material to ensure homogeneity between sample splits. Subsamples from homogenized powders were divided for major, minor, and trace element geochemistry and further subdivided for separate HSE work at LabMaTer, University of Québec at Chicoutimi, Canada. The HSE abundances of *GR97M22*, *IN05013*, *IN05019*, *IN05021*, *IN05056*, *IN08012*, *IN08016*, *IN08017*, *IN08043*, and *IN08044* were analyzed along with the OKUM (Ontario komatiite ultramafic) standard using 2 g of powdered sample in high-pressure asher digestion followed by isotope dilution. The HSE of samples *GR9703*, *GR0019*, *GR0020*, *GR0030, GR0031*, *GR04064*, *GR04065*, and *IN05047* as well as the bb-235 (LabMaTer in-house basaltic komatiite) standard were extracted using 15 g of sample by nickel–sulfur assay and Te co-precipitation.

Table 2 Whole-rock geochemistry for the mafic samples from the Nuvvuagittuq Supracrustal Belt

Sample	IN05013	IN05019	IN05021	IN05046	IN08012	IN08017	IN08043	IN08044
Locality	Nuvvuagittuq	Nuvvuagittuq	Nuvvuagittuq	Nuvvuagittuq	Nuvvuagittuq	Nuvvuagittuq	Nuvvuagittuq	Nuvvuagittuq
Age (Ma)	3750	3750	3750	3750	3750	3750	3750	3750
Reference	1, 2	1, 2	1, 2	1	3	3	3	3
SiO_2	48.88	46.27	48.87	46.27	42.78	46.56	49.21	44.94
TiO_2	0.700	0.830	0.710	0.670	0.983	0.567	0.827	0.882
Al_2O_3	15.21	15.93	15.34	16.38	14.52	15.88	16.05	15.11
MgO	9.74	9.20	8.64	9.11	12.33	12.50	9.57	12.82
Fe_2O_3	12.94	13.02	12.05	11.77	19.78	13.38	13.31	13.49
MnO	0.18	0.19	0.20	0.19	0.19	0.27	0.17	0.20
CaO	6.28	9.26	9.76	10.89	1.41	2.18	3.31	3.59
Na_2O	0.82	1.30	1.96	1.28	0.06	0.69	1.20	1.50
K_2O	2.25	1.95	0.99	1.21	3.20	2.43	2.16	1.04
P_2O_5	0.07	0.08	0.07	0.07	0.08	0.09	0.10	0.11
LOI	2.74	1.64	1.46	1.94	5.34	6.23	4.61	5.06
Total	99.8	99.7	100.1	99.8	100.7	100.8	100.5	98.7
Rb	69.6	68.3	31.2	43	130.1	82.17	73.55	40.76
Sr	62.5	63.0	73.4	108	4.513	58.04	75.67	72.15
Ba	341	293	85	139	196.2	440.3	333.3	223.2
Sc	40.0	44.04	39.05	47.3				
Nb	1.85	2.18	2.02	1.65	4.0	1.629	1.7	2.1
Ta	0.29	0.61	1.17	0.80	0.30	0.23	0.10	0.16
Y	15.70	16.90	16.55	17.9	16.31	11.45	15.44	14.81
Zr	39.5	43.6	39.9	40	81	61.77	49	49
Ni	169	143	146	180	114.8	180	135.7	149
Cr	293	398	350	512	163.3	613.5	345.3	284.1
V	232	259	243	273	308.7	144.7	218.4	250.7
Co					53.52	47.75	49.34	52.82
Cu	10	79	76	67	19	<D.L.	<D.L.	<D.L.
Zn	72	68	68	64	149	108	94	152
La	2.22	3.86	3.16	2.37	4.218	5.274	2.366	2.781
Ce	5.95	8.66	8.37	6.00	8.404	11.08	5.605	7.126
Pr	0.94	1.23	1.30	0.94	1.048	1.37	0.865	1.116
Nd	4.99	6.12	6.73	4.98	4.599	5.488	4.391	5.62
Sm	1.65	1.86	2.00	1.62	1.252	1.442	1.667	1.843
Eu	0.69	0.86	0.78	0.66	0.398	0.431	0.909	0.621
Gd	2.30	2.51	2.63	2.20	1.694	1.695	2.09	2.288
Tb	0.42	0.46	0.46	0.41	0.32	0.302	0.374	0.39
Dy	2.90	3.17	3.09	2.65	2.397	2.01	2.505	2.526
Ho	0.60	0.67	0.65	0.58	0.594	0.424	0.534	0.532
Er	1.81	1.98	1.91	1.77	1.934	1.223	1.567	1.527
Tm	0.270	0.297	0.286	0.26	0.324	0.192	0.231	0.231
Yb	1.81	1.95	1.90	1.75	2.335	1.35	1.629	1.584
Lu	0.283	0.305	0.295	0.28	0.389	0.213	0.254	0.251
Hf	1.16	1.31	1.19	1.09	2.18	1.61	1.34	1.38
Th	0.30	0.30	0.25	0.16	1.025	0.408	0.078	0.451
U	0.09	0.28	0.26	0.07	0.27	0.15	0.13	0.12
Pb	0.9	2.2	3.8	1.9	1.44	2.21	0.97	2.66

Data come from (1) Cates and Mojzsis (2007), (2) Dauphas et al. (2007), and (3) Cates et al. (2013)

Further detail for both methods are described by Savard et al. (2010), who showed that nickel–sulfur fire assay and isotope dilution high-pressure asher acid digestion produce reliable results in the analysis of Ru, Pd, Os, Ir, and Pt. Measurements for all samples were made through ICP-MS solution analysis at LabMaTer. Detail on analytical precision is provided in Supplementary online material File 1.

Results

Platinum group element abundances for the samples are reported in Table 3. Maier et al. (2009) focused on platinum as a Late Veneer tracer because many komatiites were metamorphosed to near greenschist facies, and Pt tends to be immobile under most conditions (Puchtel et al. 2014). Maier et al. (2009) also plotted Ru vs. MgO as Ru has a bulk $D_{melt/mantle}$ of approximately 1 into the mantle during komatiite production and thus may also provide a reasonable indicator of mantle Ru contents (Maier et al. 2012). Excluding *GR97M22*, which showed an unusually high abundance of Pt (35.2 ppb), the mean concentrations in our two other Innersuartuut ultramafic samples are 2.3 ± 0.3 ppb Pt and 2.9 ± 1.5 ppb Ru. Error here corresponds to standard deviation. Averages for the five Akilia Island samples are 5.9 ± 1.2 ppb Pt and 3.4 ± 0.9 ppb Ru and those for the two Nuvvuagittuq ultramafic rocks are 1.4 ± 0.6 ppb Pt and 1.6 ± 0.9 ppb Ru. The mafic samples from Nuvvuagittuq have a mean Pt of 4.4 ± 3.0 ppb. Figure 3 shows Pt, Ru, and Pd plotted against MgO. Ruthenium shows a clear positive trend as a function of MgO, but there is more scatter for Pt and Pd. The mafic suite in particular shows a large variation in Pt and Pd abundances.

Platinum is incompatible during crystallization of sulfur-undersaturated komatiite magma, and thus, Pt contents of the magma are expected to increase with degree of fractionation as seen in the global database of komatiites in Maier et al. (2009). Given that our samples have experienced different degrees of fractionation, comparing their absolute Pt abundances is not particularly instructive. As a result, to compare variably fractionated komatiites with each other and to deduce the nature of their mantle source, we normalized the Pt concentrations of our samples to 25 wt% MgO following the approach of Maier et al. (2009). The normalization is performed by either subtracting or adding olivine to a komatiite by applying the lever rule. For the ultramafic samples, we assume that olivine has the composition $Fo_{93.5}$ and 52 wt% MgO. Here, correction factor F equals (1) for a rock with >25 wt% MgO, the fraction of olivine that needs to be subtracted to bring the whole-rock composition to 25 % (2) for a rock with <25 wt% MgO, and the fraction of olivine that needs to be added to shift the liquid composition to 25 wt% MgO:

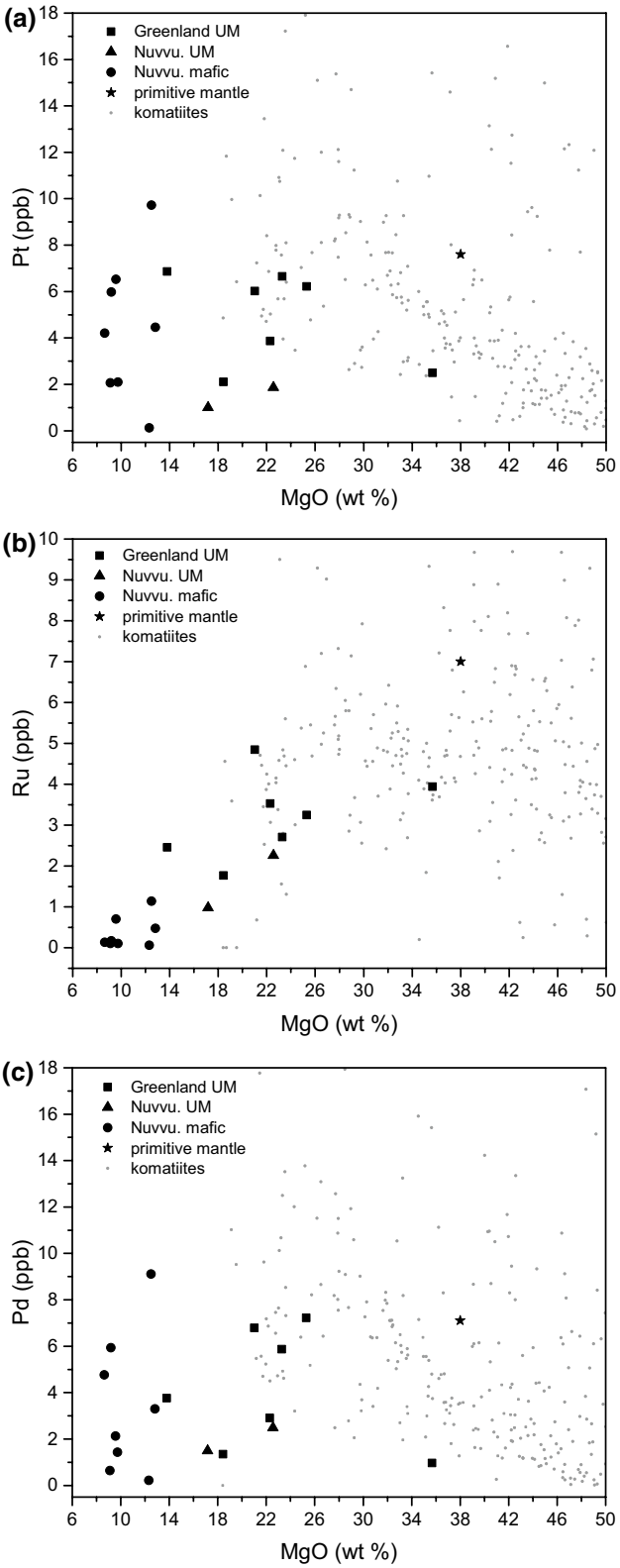

Fig. 3 **a** Pt, **b** Ru, and **c** Pd concentrations in ultramafic (UM) and mafic samples as a function of MgO wt%. *Gray points* are data from komatiites identified in Barnes and Fiorentini (2008) and Maier et al. (2009), provided in Supplementary File 2

Table 3 Highly siderophile element abundances for both ultramafic and mafic samples from all localities

Sample	Locality	MgO (wt%)	Os (ppb)	Ir (ppb)	Ru (ppb)	Pt (ppb)	Pd (ppb)	Re (ppb)	Rh (ppb)
GR0020	Akilia Island	25.3	0.813	0.729	3.246	6.217	7.221		0.844
GR0031	Akilia Island	23.28	0.557	0.597	2.706	6.650	5.866		0.871
GR9703	Akilia Island	22.29	0.74	0.69	3.53	3.87	2.91		0.90
GR0019	Akilia Island	21.03	1.236	1.190	4.848	6.019	6.789		1.053
GR0030	Akilia Island	13.8	0.43	0.575	2.460	6.867	3.760		0.997
GR04064	Innersuartuut	35.69	1.19	1.24	3.94	2.50	0.97		0.78
GR97M22	Innersuartuut	26.82	0.520	0.286	1.913	8.610	35.187	0.013	
GR04065	Innersuartuut	18.43	0.43	0.50	1.77	2.11	1.35		0.47
IN05047	Nuvvuagittuq	22.56	1.49	0.85	2.26	1.86	2.49		0.28
IN08016	Nuvvuagittuq	17.17	0.252	0.175	0.983	0.993	4.889	1.267	
IN08044	Nuvvuagittuq	12.82	0.216	0.236	0.475	4.456	3.302	1.264	
IN08017	Nuvvuagittuq	12.495	0.139	0.293	1.141	9.721	9.110	0.059	
IN08012	Nuvvuagittuq	12.328	0.116	0.007	0.061	0.118	0.222	0.175	
IN05013	Nuvvuagittuq	9.736	0.037	0.064	0.107	2.095	1.428	0.303	
IN08043	Nuvvuagittuq	9.565	0.081	0.167	0.704	6.526	2.127	0.013	
IN05019	Nuvvuagittuq	9.2	0.221	0.251	0.171	5.980	5.935	0.390	
IN05046	Nuvvuagittuq	9.11	0.029	0.065	0.102	2.064	0.635	0.405	
IN05021	Nuvvuagittuq	8.643	0.038	0.211	0.137	4.206	4.763	0.151	

Table 4 Pt and Pd abundances for ultramafic samples normalized to 25 wt% MgO using Eq. 1

Sample	Locality	MgO (wt%)	Scaling factor	Measured Pt (ppb)	Normalized Pt (ppb)	Measured Pd (ppb)	Normalized Pd (ppb)
GR0020	Akilia Island	25.3	1.011	6.217	6.287	7.221	7.302
GR0031	Akilia Island	23.28	0.940	6.650	6.252	5.866	5.515
GR9703	Akilia Island	22.29	0.909	3.87	3.52	2.91	2.64
GR0019	Akilia Island	21.03	0.872	6.019	5.247	6.789	5.919
GR0030	Akilia Island	13.8	0.707	6.867	4.854	3.760	2.658
GR04064	Innersuartuut	35.69	1.655	2.50	4.14	0.97	1.61
GR04065	Innersuartuut	18.43	0.804	2.11	1.70	1.35	1.09
IN05047	Nuvvuagittuq	22.56	0.917	1.86	1.71	2.49	2.28
IN08016	Nuvvuagittuq	17.17	0.775	0.993	0.770	4.889	3.790

$$F = \frac{52 - 25}{52 - \mathrm{MgO_{rock}}} \quad (1)$$

The concentration of Pt of a sample is multiplied by its F so that the relative abundances between samples of varying MgO can be compared. This normalization technique works best for ultrabasic liquids that have only olivine on the liquidus. It is worth pointing out that this technique also provides useful information in Mg-rich basalts such as the samples from Nuvvuagittuq because in these too olivine is by far the most important liquidus phase. Plagioclase and orthopyroxene only begin to crystallize in typical komatiitic melts at ~8.5 wt% MgO, with clinopyroxene and chromite often appearing somewhat earlier. Normalized Pt and Pd abundances are shown in Table 4.

Figure 4 shows the concentration of Pt and Ru in komatiites (Pt is normalized to 25 wt% MgO) as a function of their age. The data shown include our own and that from Maier et al. (2009) and are provided in Supplementary File 2. They were selected based on the following criteria: 15–40 wt% MgO, 0.1 < TiO_2 < 1.0, Pt/Ti < 1.5, and high-quality HSE data. Nuvvuagittuq ultramafic data from Touboul et al. (2014) for which MgO values are reported (O'Neil et al. 2007, 2011; samples PC-220 and PC-504 from that data set do not have published MgO abundances) were normalized to 25 wt% MgO and plotted using our preferred Nuvvuagittuq age of ca. 3.78 Ga from Cates and Mojzsis (2007) and Cates et al. (2013) (cf. O'Neil et al. 2008, 2012 for an age estimate of ca. 4.38 Ga). As shown in Fig. 4, our new ultramafic HSE data are broadly consistent

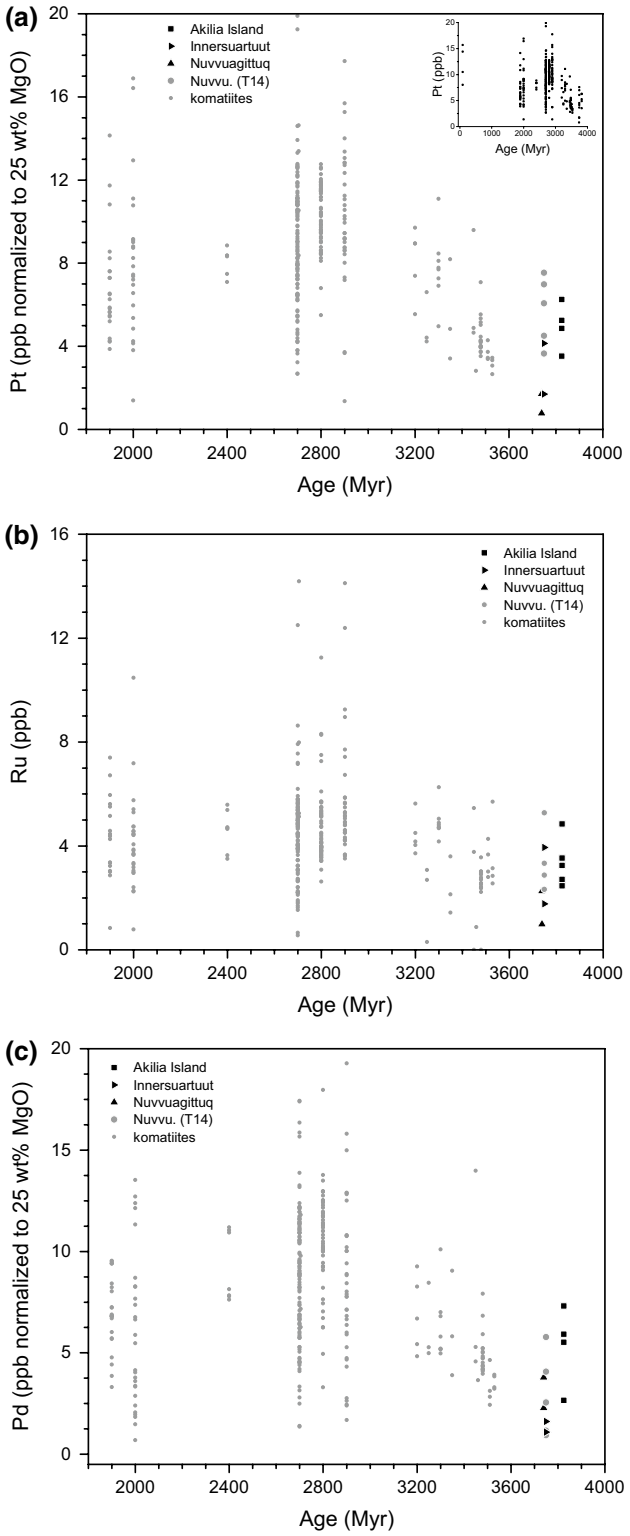

Fig. 4 **a** Pt, **b** Ru, and **c** Pd abundances versus age for our ultramafic samples along with published komatiite data. Abundances are normalized to 25 wt% MgO using Eq. 1. *Gray points* are data from komatiites identified in Barnes and Fiorentini (2008) and Maier et al. (2009), and the "Nuvvu. (T14)" samples are data from Touboul et al. (2014) using our preferred age for the Nuvvuagittuq Supracrustal Belt. The *inset* in (**a**) is the same data plus measurements from 88-Myr-old Gorgona Island komatiites (Brandon et al. 2003)

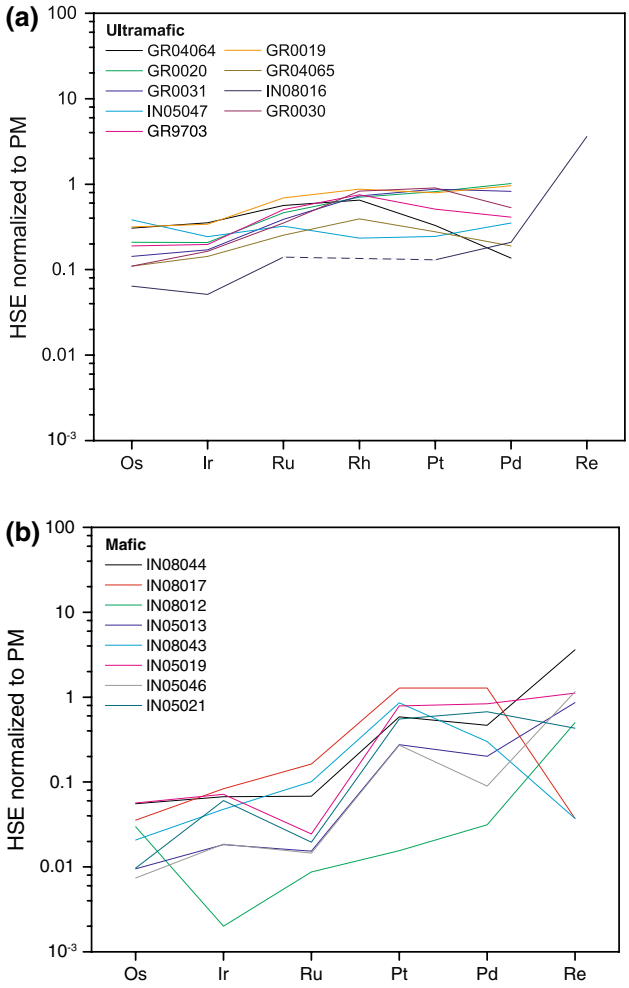

Fig. 5 HSE abundances in **a** ultramafic and **b** mafic samples normalized to primitive mantle abundances from Becker et al. (2006). Sample *GR0030* is grouped with the ultramafic samples

with the depletion trend previously observed by Maier et al. (2009) for samples older than about 3 Ga. As we discuss in the following section, our results for this depletion trend in the Eoarchean appear to be at odds with Touboul et al. (2014) for ultramafic samples from the Nuvvuagittuq supracrustal belt.

Discussion

Protolith assignment and reliability of HSE data

The key challenge faced in this work with these deformed and metamorphosed Eoarchean mafic and ultramafic rocks is that we must distinguish those of komatiitic protolith from cumulates of basaltic magmas. One possible test would be to compare forsterite contents which should be

>90 for komatiite, but <90 for basaltic cumulates, but the oldest komatiites (*s.l.*) are generally too altered for olivine to be preserved. Instead, Mouri et al. (2013) used HSE patterns to distinguish komatiites from basaltic cumulates. Basalts have more fractionated patterns than komatiites because the IPGE and Rh are more compatible than Pt and Pd during mantle melting and fractional crystallization. Basaltic cumulates tend to have less fractionated patterns than basaltic magmas due to compatibility of IPGE into olivine and chromite (Mungall and Brenan 2014), but the cumulates rarely have smooth unfractionated patterns as in komatiites, due to strong nugget effects during fractional crystallization.

The HSE patterns in Fig. 5a for the ultramafic samples are relatively flat, consistent with that of previously identified komatiites (e.g., Fiorentini et al. 2011), whereas the PGE patterns of the mafic samples (Fig. 5b) are more fractionated, resembling typical basalts (Barnes et al. 2015). Komatiitic basalt *GR0030* is an exception as it has more fractionated patterns than the more mafic samples.

A further test to distinguish komatiites from basaltic cumulates is to consider Cr contents. (Fig. 6). Basaltic cumulates have highly variable and often have higher Cr contents than komatiite liquids as the latter are mostly Cr-undersaturated (Barnes and Fiorentini 2008). Our ultramafic samples fall on the komatiite trend, while most mafic samples hover at around the MORB value for Cr (357.1 ppm; Kelemen et al. 2004) and plot broadly along the trend of global basalts.

Mungall and Brenan (2014) have found that Pt contents of basalts can be affected by oxygen fugacity and depth of melting, with fO_2 and thus Pt alloy solubility increasing with depth. They used this argument to explain the relatively high Pt/Pd of Bushveld basaltic magmas. It is worth pointing out, however, that this is unlikely to have significantly affected the Pt content of komatiites based on the observation that global komatiites show relatively constant Pt/Pd, with the exception of Karasjok komatiites (Fiorentini et al. 2011).

Another way to check whether our Eoarchean ultramafic supracrustal samples were komatiite melts rather than basaltic cumulates is to evaluate them on the basis of their Ti and Al abundances (e.g., Fiorentini et al. 2011). Figure 7 shows all samples in a plot of Ti versus Al compared to the komatiite database of Fiorentini et al. (2011). The ultramafic Greenland (Akilia Island and Innersuartuut) samples in our suite fall below the main trend, and the Nuvvuagittuq samples fall above, but it should be noted that all are within the scatter of recorded komatiitic values. The particularly high-Ti Nuvvuagittuq sample is IN08016, which we previously identified as a basaltic komatiite on the basis of its geologic context. The mafic Nuvvuagittuq samples are high in both Al and Ti, consistent with basalts.

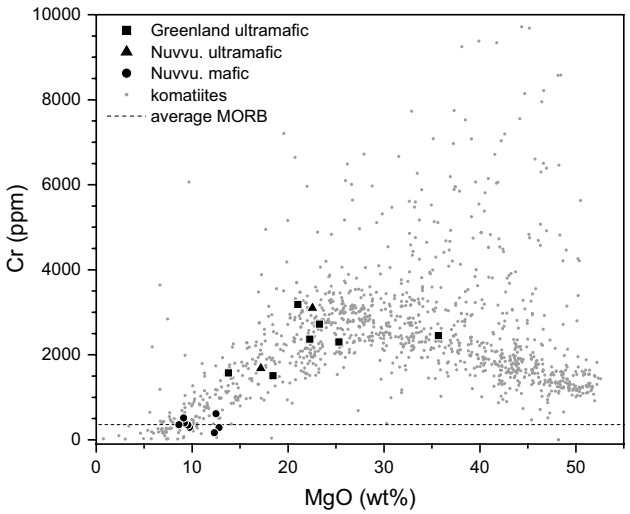

Fig. 6 Chromium abundances of the Nuvvuaqittuq ("Nuvvu.") ultramafic and mafic samples and Greenland (Akilia Island and Innersuartuut localities) ultramafic samples relative to average MORB (Kelemen et al. 2004) and komatiites from the database of Fiorentini et al. (2011)

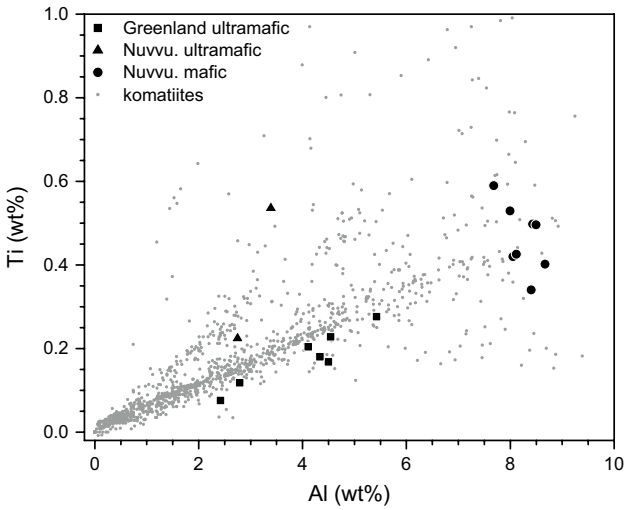

Fig. 7 Ti versus Al data for the samples presented here compared to the komatiite database of Fiorentini et al. (2011). The Greenland samples include those from the Akilia Island and Innersuartuut localities

Overall, we interpret the Akilia Island and Innersuartuut samples from Greenland to be komatiitic in origin. On the other hand, the highly variable PGE and high Ti of the Nuvvuagittuq ultramafic samples are more difficult to interpret. We cannot rule out the possibility that these samples may be basalts with a cumulate component or that they experienced metamorphism that resulted in HSE mobility or Pt alloy saturation. Some of the mafic Nuvvuagittuq samples show particularly depleted HSE in an otherwise inconsistent field of values, which also include some anomalously

high concentrations (cf. Touboul et al. 2014). We interpret this to mean that the Nuvvuagittuq HSE results are unlikely to be representative of their source. Consequently, we view our oldest Eoarchean samples from West Greenland's Akilia association as providing the best measure of pre-Late Veneer mantle HSE abundances.

A signature of the pre-Late Veneer terrestrial mantle?

The ultramafic HSE data reported here are consistent with the low HSE abundances of Archean samples analyzed by Maier et al. (2009), but our Nuvvuagittuq samples may have experienced HSE depletion during emplacement. Touboul et al. (2014) presented the results of HSE analyses for selected Nuvvuagittuq samples of ultramafic, mafic, and tonalitic composition. The results of their ultramafic samples are of particular interest here in our evaluation of the record of the Late Veneer signature in komatiites. The authors reported mean concentrations of 8.6 ± 7.9 ppb Pt (2σ standard deviation) in the mafic samples and 5.1 ± 4.5 ppb Pt in the ultramafic samples. (The ultramafic mean excludes two outlier samples with anomalously high Pt, approximately 20 ppb.) Their mafic samples are higher in HSE and less variable than those we report. Our Nuvvuagittuq samples, in combination with those of Touboul et al. (2014), indicate that the mafic components of the belt are variable in their HSE abundances and that mafic samples need to be carefully scrutinized to establish their suitability as HSE tracers of the Late Veneer.

While the ultramafic abundances reported in Touboul et al. (2014) are somewhat higher than those presented here, normalizing them to 25 wt% MgO shows them to be broadly consistent with that of other Archean komatiites (Fig. 4). The authors favor an alternate interpretation, however, in which their reported abundances are approximately that of the modern-day mantle. The mantle convection model allows for outliers: it is entirely to be expected that some younger komatiites may be PGE-depleted, or some older ones relatively enriched. Alternatively, it is possible that mantle mixing was incomplete in the Archean, and the komatiite source was heterogeneous, and/or there were independent mixing mechanisms such as subduction or plume ascent as opposed to intra-mantle convection. Our preferred interpretation is that the Greenland results presented here are consistent with ^{142}Nd and ^{182}W observations and models for protracted mantle mixing on the early Earth as described in the next section.

Archean "trickle-down" geodynamics

The notion of long and slow mantle mixing is an important component to the "trickle-down geodynamics" (Arndt 2009) concept put forth in Maier et al. (2009). Once the Late Veneer material reached Earth, it must have been stored in an upper mantle domain, and the komatiite reservoir(s) started off with near-negligible HSE abundances that later become contaminated as mixing progressed. At approximately 3 Ga (Fig. 4), roughly modern-day peridotite HSE abundances are reached. If this interpretation is correct, by around 3 Ga, HSE pollutants from the upper mantle were well mixed into the deep-mantle komatiite reservoir. We note that this is broadly consistent with the approximately 750-Myr mixing time suggested by μ^{142}Nd measurements from Eoarchean rocks (e.g., Bennett et al. 2007; Carlson and Boyet 2008; Roth et al. 2014) but is tenfold slower than that expected in convection models, which lead to homogenization in less than ~100 Myr (Caro et al. 2006; Coltice and Schmalzl 2006). Recent analysis of a tholeiitic lava flow in the Abitibi Greenstone Belt (2.7 Ga) showed a positive μ^{142}Nd anomaly, which Debaille et al. (2013) argued was evidence of a major geodynamical regime switch at about 3 Ga from stagnant-lid to mobile-lid plate tectonics. This is also about the same time that HSE komatiite abundances appear to level off in our data. Furthermore, the positive ε^{182}W anomalies presented by Willbold et al. (2011) for the Eoarchean Isua Supracrustal Belt in West Greenland, the Acasta Gneiss Complex in Canada (Willbold et al. 2015), and from Touboul et al. (2012) for rocks as young as 2.8 Ga (Kostomuksha komatiites) provide additional evidence that the early mantle did not rapidly convect to the degree that it was able to eradicate primordial heterogeneities.

The Sm–Nd system provides information on mantle mixing rates as well as what exactly was being mixed. Neodymium-142 excesses in rocks from the Isua Supracrustal Belt in West Greenland show that they were derived from a Hadean mantle depleted in highly incompatible elements (Boyet et al. 2003; Caro et al. 2006). The initial depletion of the early mantle would have occurred shortly after Earth's formation as a result of global magma ocean differentiation or extraction followed by isolation of primordial crust. A differentiation event that formed the Isua depleted reservoir would have also formed a complementary enriched reservoir. Evidence for this was found in mafic dikes and the idea that mantle heterogeneities could be preserved until at least 3.4 Ga (Rizo et al. 2012). New combined Lu–Hf and Sm–Nd results from the Acasta Gneiss Complex show that the Hadean crust was reworked and ultimately destroyed after a residence time of about 1.5 Gyr (Guitreau et al. 2014; Roth et al. 2014).

Komatiites can provide further information on the postulated complementary Hadean reservoirs. Specifically, Sm/Nd and Lu/Hf ratios in early Archean komatiites are lower than those in Proterozoic komatiites, which suggests that an enriched reservoir and a depleted reservoir were mixed over time (Blichert-Toft and Puchtel 2010). These isotopic

systems, as well as those of Rb–Sr and O, have been interpreted to mean that the rate of continent growth was two-staged (Jacobsen 1988; Dhuime et al. 2012). It was further argued by Dhuime et al. (2012) that Earth initially experienced a high rate of continental crust growth for the first ~1.5 Gyr, but at ca. 3 Ga there was a decline. This drop may have been due to a shift in how continents are made and preserved as the mantle transitioned to modern-day subduction-driven plate tectonics. Coincidentally, it is during this same time that Pt and Ru abundances in komatiites (Fig. 4) appear to level off to approximately modern concentrations. The HSE may be an additional independent marker of a global shift in mantle behavior and mixing between reservoirs.

The Late Veneer source

Geochemical analyses cannot currently differentiate between the impact of a single large projectile and multiple impacts of smaller bodies, although constraints can be generated via geophysical limitations and dynamical likelihood. For example, a single large planetary object that is 2500–3000 km in diameter and formed early in solar system history is large enough to be differentiated (McSween et al. 2002). In such a case, its HSE should be sequestered in its core. Based on our current state of knowledge, the number of suitably large impactors at the time of the LV (Fig. 1) was probably small. A further requirement is that if such a large impactor hit Earth, the HSE lodged within the projectile's core somehow stayed suspended in Earth's mantle. The dynamical modeling results of Bottle et al. (2010) make this hypothesis plausible had the strike been a "hit-and-almost-run" event that ended up shattering the impactor's core as it collided with Earth. In this scenario, a spiral of debris around Earth rains back down to the surface (Asphaug 2010). This is a mechanism worth exploring with future impact modeling. We expect that the upper mantle can be polluted with the impactor core material while keeping the impactor HSE away from Earth's core.

A multiple impactor scenario is also feasible within presently known parameters. The Late Veneer could have arrived through a fleet of small, oxidized bodies had sufficient mass been available in the source region to provide for this flux. The multiple impactor scenario also removes the problem of keeping a large impactor core away from Earth's core. The multiple impactor solution, however, introduces a problem of numbers. Were there enough small impactors available to deliver up to ~0.5 % Earth's current mass so late in solar system history? For reference, the asteroid belt is ~0.06 % M_{Earth} (Krasinsky 2002). The late accretion Earth/Moon impactor flux ratio was ~800–1200, but those for both late-accreting planetesimals and present near-Earth objects are nearly 20 (Bottke 2002; Bottke et al. 2007; Nesvorný et al. 2010) and about 50 for micrometeorites (Nesvorný et al. 2010), respectively. In their dynamical simulations of potential late accretion impactors, Bottke et al. (2010) explored the parameter space of plausible impactor flux ratios that depend on timing and impactor composition, concluding that the stochastic nature of large impacts such as the Late Veneer is the most viable explanation for the anomalous impactor flux ratio. More work is warranted on this topic.

Evidence exists for late accretion on other planetary bodies. The delivery of extraterrestrial material is the simplest explanation for the chondritic relative proportions measured in samples from Earth and the Moon (Kruijer et al. 2015; Touboul et al. 2015), although a hybrid model incorporating more than one explanation for the HSE enrichment is not inconsistent with those observations (Kramers 1998; Rubie et al. 2003; Mann et al. 2012; Wang and Becker 2013). Pinning down the precise origin of Earth's Late Veneer is elusive, but solar system-wide evidence for a period of late accretion lends support from beyond Earth to the Late Veneer hypothesis.

Late Veneer versus Late Heavy Bombardment

The Late Veneer, if it were an event at the tail end of planetary accretion, must have occurred after the final large-scale impact to the burgeoning Earth that induced effective metal-silicate equilibration between mantle and core (Kimura et al. 1974). It is widely accepted that this event happened with the postulated Moon-forming impact some 60–100 Myr into solar system history (e.g., Rudge et al. 2010; Jacobsen et al. 2014). A giant impact to the proto-Earth is thought to have generated a debris disk that re-accreted to form the Moon (e.g., Canup and Asphaug 2001; Canup 2004, 2008; Ćuk and Stewart 2012). Any accretion events preceding the Moon's formation that variably enriched Earth's mantle with HSE are expected to have had that signature erased owing to disruption and reformation of Earth's core (Leinhardt and Stewart 2012). With this in mind, we postulate that the time frame of about 4.50–4.37 Ga can be used as loose temporal bounds for when the LV was delivered to Earth. The late lower bound is provided by the oldest U–Pb ages obtained from detrital zircons of the Jack Hills outcrops within the Narryer Gneiss Complex of Western Australia (Harrison 2009; Valley et al. 2014).

In comparison, a late lunar cataclysm (Tera et al. 1974), or as it is more commonly termed, the "Late Heavy Bombardment" (hereafter, LHB), substantially *post-dated* the LV and was relatively far less violent (Abramov and Mojzsis 2009; Morbidelli et al. 2012; Abramov et al. 2013; Norman and Nemchin 2014; Hopkins and Mojzsis 2015).

Calculations show that the LHB had the potential to melt upwards of 5 vol% of Earth's crust down over 4 km in depth and that it had a cumulative delivered mass of about 1.8×10^{20} kg (Abramov and Mojzsis 2009): this is 1500× less than that estimated for the Late Veneer provided by Walker (2009). Although it is evident that the delivery of the LHB to Earth was enough to cause regional-scale damage to the crust, these effects were trivial with respect to the bulk chemistry of the silicate Earth. Conflating the Late Veneer and the Late Heavy Bombardment as related events severely misconstrues interpretations of the HSE data in the context of late accretion. At minimum, a roughly 20× increase in cumulative impactor mass from the LHB baseline flux (Abramov and Mojzsis 2009) is enough to destroy the entire volume of Earth's crust down to the lithospheric mantle (Abramov et al. 2013). Late Veneer-scale events hundreds of times greater than this are expected to have not only disrupted and melted the surface, but also to have led to formation of shallow (~50–200 km deep) magma seas that had the capacity to effectively fuse the crust and reset radiogenic systems (e.g., Elkins-Tanton 2008; Marchi et al. 2014).

Conclusions

Late accretion is a process that any young planetary body in our solar system experienced following differentiation. Earth's geological activity has erased nearly all tangible records of its earliest history, but the Late Veneer signature can be read in the HSE abundances of ancient komatiites. We interpret these to record mixing of primordial HSE pollutants into the deep mantle. New data for >3.7 Ga ultramafic rocks from the Nuvvuagittuq and Akilia localities extend this record back to the oldest known rocks of komatiite protolith and complement the recent PGE and W-isotope analyses from Nuvvuagittuq by (Touboul et al. 2014). Eoarchean mafic and ultramafic rocks show depletions of HSE that are lower than the average younger komatiite as well as primitive mantle. We cannot rule out the influence of metamorphism or cumulate components on some of the Nuvvuagittuq samples, showing the challenges inherent in analyzing such ancient, metamorphosed rocks for their HSE abundances.

Highly siderophile element analyses of Eoarchean komatiite-like rocks are limited by scarce sample availability from the oldest supracrustal belts. Indeed, few HSE data exist for the time period between 2.9 and 3.1 Ga (Fig. 4) due to a lack of availability of komatiites of that age. Additional tests of the model advocated herein can be made by searching and analyzing for yet more Eoarchean and mid-Archean komatiites; one possibility includes the 3.35 Ga komatiites of the Dharwar craton in India (Jayananda et al. 2008). We predict that future samples will confirm the inferred trends described in this work and extending the komatiite record further back in time will show the continuation of a progressive decrease in deep-mantle HSE concentrations. We also recognize that this model permits outliers. It may very well be that for Earth, the Late Veneer lies on the impact-scale continuum between the giant impact that formed the Moon and the Late Heavy Bombardment. The Late Veneer is yet another milestone for planetary maturation in the construction of our solar system.

Acknowledgments We have benefitted from discussions and debates on the topics presented herein with (in alphabetical order): N. Arndt, W. Bottke, R. Brasser, S. Marchi, A. Morbidelli, R. Walker, S. Werner, and M. Willbold. We further thank N. Arndt for his constructive comments on an earlier version of this manuscript. We also thank S.-J. Barnes and D. Savard at the Université du Québec à Chicoutimi for performing the HSE analyses. E.A.F. was supported by a NASA Earth and Space Science Fellowship (NESSF), "Exploring the Darkest of the Dark Ages," and the Zonta International Amelia Earhart Fellowship. S.J.M. acknowledges support from the NASA Lunar Science Institute through the Center for Lunar Origin and Evolution (CLOE) and the NASA Exobiology Program. A substantial portion of this manuscript was completed while S.J.M. held a Distinguished Research Professorship in Budapest at the Research Center for Astronomy and Earth Sciences of the Hungarian Academy of Sciences. This is a contribution of the Collaborative for Research in Origins (CRiO), which is funded by the John Templeton Foundation.

References

Abramov O, Mojzsis SJ (2009) Microbial habitability of the Hadean Earth during the late heavy bombardment. Nature 459:419–422

Abramov O, Kring DA, Mojzsis SJ (2013) The impact environment of the Hadean Earth. Chem Erde Geochem 73:227–248

Anbar AD, Zahnle KJ, Arnold GL, Mojzsis SJ (2001) Extraterrestrial iridium, sediment accumulation and the habitability of the early Earth's surface. J Geophys Res 106:3219

Arndt N (2003) Komatiites, kimberlites, and boninites. J Geophys Res 108:2293

Arndt N (2009) Earth science: trickle-down geodynamics. Nature 460:583–584

Arndt NT, Naldrett AJ, Pyke DR (1977) Komatiitic and iron-rich tholeiitic lavas of Munro Township, Northeast Ontario. J Petrol 18:319–369

Arndt N, Lesher CM, Barnes SJ (2008) Komatiite. Cambridge University Press, Cambridge

Asphaug E (2010) Similar-sized collisions and the diversity of planets. Chem Erde Geochem 70:199–219

Barnes SJ, Fiorentini M (2008) Iridium, ruthenium and rhodium in komatiites: evidence for iridium alloy saturation. Chem Geol 257:44–58

Barnes S-J, Naldrett A, Gorton M (1985) The origin of the fractionation of platinum-group elements in terrestrial magmas. Chem Geol 53:303–323

Barnes SJ, Mungall JE, Maier WD (2015) Platinum group elements in mantle melts and mantle samples. Lithos 232:395–417

Bennett VC, Brandon AD, Nutman AP (2007) Coupled ^{142}Nd–^{143}Nd isotopic evidence for Hadean mantle dynamics. Science 318:1907–1910

Blichert-Toft J, Puchtel IS (2010) Depleted mantle sources through time: evidence from Lu–Hf and Sm–Nd isotope systematics of Archean komatiites. Earth Planet Sci Lett 297:598–606

Bottke W (2002) Debiased orbital and absolute magnitude distribution of the near-Earth objects. Icarus 156:399–433

Bottke WF, Levison HF, Nesvorný D, Dones L (2007) Can planetesimals left over from terrestrial planet formation produce the lunar Late Heavy Bombardment? Icarus 190:203–223

Bottke WF, Walker RJ, Day JMD, Nesvorný D, Elkins-Tanton E (2010) Stochastic late accretion to Earth, the Moon, and Mars. Science 330:1527–1530

Boyet M, Blichert-Toft J, Rosing M, Storey M, Télouk Albarède (2003) ^{142}Nd evidence for early Earth differentiation. Earth Planet Sci Lett 214:427–442

Brandon AD, Walker RJ, Puchtel IS, Becker H, Humayun M, Revillon S (2003) ^{186}Os–^{187}Os systematics of Gorgona Island komatiites: implications for early growth of the inner core. Earth Planet Sci Lett 206:411–426

Canup RM (2004) Simulations of a late lunar-forming impact. Int J Sol Syst Stud 168:433–456

Canup R (2008) Lunar-forming collisions with pre-impact rotation. Icarus 196:518–538

Canup RM, Asphaug E (2001) Origin of the Moon in a giant impact near the end of the Earth's formation. Nature 412:708–712

Carlson RW, Boyet M (2008) Composition of the Earth's interior: the importance of early events. Philos Trans A Math Phys Eng Sci 366:4077–4103

Caro G, Bourdon B, Birck J-L, Moorbath S (2006) High-precision ^{142}Nd/^{144}Nd measurements in terrestrial rocks: constraints on the early differentiation of the Earth's mantle. Geochim Cosmochim Acta 70:164–191

Cates NL, Mojzsis SJ (2006) Chemical and isotopic evidence for widespread Eoarchean metasedimentary enclaves in southern West Greenland. Geochim Cosmochim Acta 70:4229–4257

Cates NL, Mojzsis SJ (2007) Pre-3750 Ma supracrustal rocks from the Nuvvuagittuq supracrustal belt, northern Québec. Earth Planet Sci Lett 255:9–21

Cates NL, Mojzsis SJ (2009) Metamorphic zircon, trace elements and Neoarchean metamorphism in the ca. 3.75 Ga Nuvvuagittuq supracrustal belt, Québec (Canada). Chem Geol 261:99–114

Cates NL, Ziegler K, Schmitt AK, Mojzsis SJ (2013) Reduced, reused and recycled: detrital zircons define a maximum age for the Eoarchean (ca. 3750–3780 Ma) Nuvvuagittuq Supracrustal Belt, Québec (Canada). Earth Planet Sci Lett 362:283–293

Chou CL (1978) Fractionation of siderophile elements in the Earth's upper mantle. In: Proceedings of the 9th Lunar and Planetary Science Conference, Houston, TX, pp 219–230

Coltice N, Schmalzl J (2006) Mixing times in the mantle of the early Earth derived from 2-D and 3-D numerical simulations of convection. Geophys Res Lett 33:L23304

Ćuk M, Stewart ST (2012) Making the Moon from a fast-spinning Earth: a giant impact followed by resonant despinning. Science 338:1047–1052

Dahl TW, Stevenson DJ (2010) Turbulent mixing of metal and silicate during planet accretion: and interpretation of the Hf-W chronometer. Earth Planet Sci Lett 295:177–186

Dauphas N, Cates NL, Mojzsis SJ, Busigny V (2007) Identification of chemical sedimentary protoliths using iron isotopes in the >3750 Ma Nuvvuagittuq supracrustal belt, Canada. Earth Planet Sci Lett 254:358–376

Debaille V, O'Neill C, Brandon AD, Haenecour P, Yin Q-Z, Mattielli N, Treiman AH (2013) Stagnant-lid tectonics in early Earth revealed by ^{142}Nd variations in late Archean rocks. Earth Planet Sci Lett 373:83–92

Dhuime B, Hawkesworth CJ, Cawood PA, Storey CD (2012) A change in the geodynamics of continental growth 3 billion years ago. Science 335:1334–1336

Echeverría LM (1980) Tertiary or Mesozoic komatiites from Gorgona Island, Colombia: field relations and geochemistry. Contrib Mineral Petrol 73:253–266

Elkins-Tanton LT (2008) Linked magma ocean solidification and atmospheric growth for Earth and Mars. Earth Planet Sci Lett 271:181–191

Fiorentini ML, Barnes SJ, Maier WD, Burnham OM, Heggie G (2011) Global variability in the platinum-group element contents of komatiites. J Petrol 52:83–112

Green DH (1975) Genesis of Archean peridotitic magmas and constraints on Archean geothermal gradients and tectonics. Geology 3:15–18

Grove TL, Parman SW, Dann JC (1999) Conditions of magma generation for Archean komatiites from the Barberton Mountainland, South Africa. In: Fei Y, Bertka CM, Mysen BO (eds) Mantle petrology: field observations and high pressure experimentation: a tribute to Francis R. (Joe) Boyd. The Geochemical Society, Houston, pp 155–167

Guitreau M, Blichert-Toft J, Mojzsis SJ, Roth ASG, Bourdon B, Cates NL, Bleeker W (2014) Lu–Hf isotope systematics of the Hadean-Eoarchean Acasta Gneiss Complex (Northwest Territories, Canada). Geochim Cosmochim Acta 135:251–269

Halliday AN (2008) A young Moon-forming giant impact at 70–110 million years accompanied by late-stage mixing, core formation and degassing of the Earth. Philos Trans R Soc A Math Phys Eng Sci 366:4163–4181

Hanski E, Walker RJ, Huhma H, Polyakov GV, Balykin PA, Hoa TT, Phuong NT (2004) Origin of the Permian-Triassic komatiites, northwestern Vietnam. Contrib Mineral Petrol 147:453–469

Harrison TM (2009) The Hadean crust: evidence from >4 Ga Zircons. Annu Rev Earth Planet Sci 37:479–505

Herzberg C, Condie K, Korenaga J (2010) Thermal history of the Earth and its petrological expression. Earth Planet Sci Lett 292:79–88

Hopkins MD, Mojzsis SJ (2015) A protracted timeline for lunar bombardment from mineral chemistry, Ti thermometry and U–Pb geochronology of Apollo 14 melt breccia zircons. Contrib Mineral Petrol 169:30

Jacobsen SB (1988) Isotopic and chemical constraints on mantle–crust evolution. Geochim Cosmochim Acta 52:1341–1350

Jayananda M, Kano T, Peucat J-J, Channabasappa S (2008) 3.35 Ga komatiite volcanism in the western Dharwar craton, southern India: constraints from Nd isotopes and whole-rock geochemistry. Precambrian Res 162:160–179

Kelemen P, Kikawa E, Miller D (2004) Proceedings of the Ocean Drilling Program, Initial Reports, vol 209 (online)

Kimura K, Lewis RS, Anders E (1974) Distribution of gold and rhenium between nickel–iron and silicate melts: implications for the abundance of siderophile elements on the Earth and Moon. Geochim Cosmochim Acta 38:683–701

Kramers JD (1998) Reconciling siderophile element data in the Earth and Moon, W isotopes and the upper lunar age limit in a simple model of homogeneous accretion. Chem Geol 145:461–478

Krasinsky G (2002) Hidden mass in the asteroid belt. Icarus 158:98–105

Kruijer TS, Kleine T, Fischer-Gödde M, Sprung P (2015) Lunar tungsten isotopic evidence for the late veneer. Nature 520:534–537

Leinhardt ZM, Stewart ST (2012) Collisions between gravity-dominated bodies. I. Outcome regimes and scaling laws. Astrophys J 745:79

Lesher CM, Keays RR (2002) Komatiite-associated Ni–Cu–PGE deposits—Geology, mineralogy, geochemistry, and genesis. In: Cabri LJ (ed) The geology, geochemistry, mineralogy and mineral beneficiation of the platinum-group elements, Special vol 54. Canadian Institute of Mining, Metallurgy, and Petroleum, Montreal, pp 579–617

Maier WD, Barnes SJ, Campbell IH, Fiorentini ML, Peltonen P, Barnes S-J, Smithies RH (2009) Progressive mixing of meteoritic veneer into the early Earth's deep mantle. Nature 460:620–623

Maier WD, Peltonen P, McDonald I, Barnes SJ, Barnes S-J, Hatton C, Vijoen F (2012) The concentration of platinum-group elements and gold in southern African and Karelian kimberlite-hosted mantle xenoliths: implications for the noble metal content of the Earth's mantle. Chem Geol 302–303:119–135

Mann U, Frost DJ, Rubie DC, Becker H, Audétat (2012) Partitioning of Ru, Rh, Pd, Re, Ir and Pt between liquid metal and silicate at high pressures and high temperatures: implications for the origin of highly siderophile element concentrations in the Earth's mantle. Geochim Cosmochim Acta 84:593–613

Manning CE, Mojzsis SJ, Harrison TM (2006) Geology, age and origin of supracrustal rocks at Akilia, West Greenland. Am J Sci 306:303–366

Marchi S, Bottke WF, Elkins-Tanton LT, Bierhaus M, Wuennemann Morbidelli A, Kring DA (2014) Widespread mixing and burial of Earth's Hadean crust by asteroid impacts. Nature 511:578–582

McGregor V, Mason B (1977) Petrogenesis and geochemistry of metabasaltic and metasedimentary enclaves in the Amitsoq gneisses, West Greenland. Am Mineral 62:887–904

McLennan S, Taylor S, McGregor V (1984) Geochemistry of Archean metasedimentary rocks from West Greenland. Geochim Cosmochim Acta 48:1–13

McSween H Jr, Ghosh A, Grimm RE, Wilson L, Young ED (2002) Thermal evolution models of asteroids. In: Bottke WF, Cellino A, Paolicchi P, Binzel RP (eds) Asteroids III. University of Arizona Press, Tuscon, AZ, pp 559–571

Morbidelli A, Lunine JI, O'Brien DP, Raymond SN, Walsh KJ (2012) Building terrestrial planets. Annu Rev Earth Planet Sci 40:251–275

Mouri H, Maier WD, Brandl G (2013) On the possible occurrence of komatiites in the Archean high-grade polymetamorphic central zone of the Limpopo Belt, South Africa. S Afr J Geol 116:55–66

Mungall JE, Brenan JM (2014) Partitioning of platinum-group elements and Au between sulfide liquid and basalt and the origins of mantle–crust fractionation of the chalcophile elements. Geochim Cosmochim Acta 125:265–289

Nesvorný D, Jenniskens P, Levison HF, Bottke WF, Vokrouhlický (2010) Cometary origin of the zodiacal cloud and carbonaceous micrometeorites. Implications for hot debris disks. Astrophys J 713:816–836

Norman MD, Nemchin AA (2014) A 4.2 billion year old impact basin on the Moon: U–Pb dating of zirconolite and apatite in lunar melt rock 67955. Earth Planet Sci Lett 388:387–398

Nutman AP, McGregor VR, Friend CRL, Bennett VC, Kinny PD (1996) The Itsaq Gneiss complex of southern West Greenland; the world's most extensive record of early crustal evolution (3900–3600 Ma). Precambrian Res 78:1–39

O'Neil J, Maurice C, Stevenson RK, Larocque J, Cloquet C, David J, Francis D (2007) The geology of the 3.8 Ga Nuvvuagittuq (Porpoise Cove) greenstone belt, northeastern Superior Province, Canada. In: Kranendonk VMJ, Smithies RH, Bennett V (eds) Earth's oldest rocks. Elsevier, Amsterdam, pp 219–254

O'Neil J, Carlson RW, Francis D, Stevenson RK (2008) Neodymium-142 evidence for Hadean mafic crust. Science 321:1828–1831

O'Neil J, Francis D, Carlson RW (2011) Implications of the Nuvvuagittuq greenstone belt for the formation of Earth's early crust. J Petrol 52:985–1009

O'Neil J, Carlson RW, Paquette J-L, Francis D (2012) Formation age and metamorphic history of the Nuvvuagittuq Greenstone Belt. Precambrian Res 220–221:23–44

O'Neill C, Debaille V, Griffin W (2013) Deep earth recycling in the Hadean and constraints on surface tectonics. Am J Sci 313:912–932

Puchtel IS, Walker RJ, Touboul M, Nisbet EG, Byerly GR (2014) Insights into early Earth from the Pt–Re–Os isotope and highly siderophile element abundance systematics of Barberton komatiites. Geochim Cosmochim Acta 125:394–413

Richter FM (1988) A major change in the thermal state of the Earth at the Archean–Proterozoic boundary: consequences for the nature and preservation of continental lithosphere. J Petrol Spec 1:39–52

Righter K, Danielson LR, Pando KM, Williams J, Humayun M, Hervig RL, Sharp TG (2015) Highly siderophile element (HSE) abundances in the mantle of Mars are due to core formation at high pressure and temperature. Meteorit Planet Sci 50:604–631

Rizo H, Boyet M, Blichert-Toft J, O'Neil J, Rosing MT, Paquette J-L (2012) The elusive Hadean enriched reservoir revealed by ^{142}Nd deficits in Isua Archaean rocks. Nature 491:96–100

Rizo H, Walker RJ, Carlson RW, Touboul M, Horan MF, Puchtel IS, Boyet M, Rosing MT (2016) Early Earth differentiation investigated through ^{142}Nd, ^{182}W, and highly siderophile element abundances in samples from Isua, Greenland. Geochim Cosmochim Acta 175:319–336

Roth ASG, Bourdon B, Mojzsis SJ, Rudge JF, Guitreau M, Blichert-Toft J (2014) Combined ^{147,146}Sm–^{143,142}Nd constraints on the longevity and residence time of early terrestrial crust. Geochem Geophys Geosyst 15:2329–2345

Rubie DC, Melosh HJ, Reid JE, Liebske C, Righter K (2003) Mechanisms of metal–silicate equilibration in the terrestrial magma ocean. Earth Planet Sci Lett 205:239–255

Rubie DC, Frost DJ, Mann U, Asahara Y, Nimmo F, Tsuno K, Kegler P, Holzeid A, Palme H (2011) Heterogeneous accretion, composition and core–mantle differentiation of the Earth. Earth Planet Sci Lett 301:31–42

Rudge JF, Kleine T, Bourdon B (2010) Broad bounds on Earth's accretion and core formation constrained by geochemical models. Nat Geosci 3:439–443

Savard D, Barnes S-J, Meisel T (2010) Comparison between nickel–sulfur fire assay Te Co-precipitation and isotope dilution with high-pressure asher acid digestion for the determination of platinum-group elements, rhenium, and gold. Geostand Geoanalytical Res 34:281–291

Stevenson D (1981) Models of the Earth's core. Science 214:611–618

Tera F, Papanastassiou D, Wasserburg G (1974) Isotopic evidence for a terminal lunar cataclysm. Earth Planet Sci Lett 22:1–21

Touboul M, Puchtel IS, Walker RJ (2012) ^{182}W evidence for long-term preservation of early mantle differentiation products. Science 335:1065–1069

Touboul M, Liu J, O'Neil J, Puchtel IS, Walker RJ (2014) New insights into the Hadean mantle revealed by ^{182}W and highly siderophile element abundances of supracrustal rocks from the Nuvvuagittuq Greenstone Belt, Quebec, Canada. Chem Geol 383:63–75

Touboul M, Puchtel IS, Walker RJ (2015) Tungsten isotopic evidence for disproportional late accretion to the Earth and Moon. Nature 520:530–533

Valley JW, Cavosie AJ, Ushikubo T, Reinhard DA, Lawrence DF, Larson DJ, Clifton PH, Kelly TF, Wilde SA, Moser DE, Spicuzza MJ (2014) Hadean age for a post-magma-ocean zircon confirmed by atom-probe tomography. Nat Geosci 7:219–223

Viljoen M, Viljoen R (1969) The geology and geochemistry of the lower ultramafic unit of the Onverwacht Group and a proposed new class of igneous rocks. Geol Soc S Afr Spec Publ 2:55–86

Walker RJ (2009) Highly siderophile elements in the Earth, Moon and Mars: update and implications for planetary accretion and differentiation. Chem Erde Geochem 69:101–125

Walsh KJ, Morbidelli A, Raymond SN, O'Brien DP, Mandell AM (2011) A low mass for Mars from Jupiter's early gas-driven migration. Nature 475:206–209

Wang Z, Becker H (2013) Ratios of S, Se and Te in the silicate Earth require a volatile-rich late veneer. Nature 499:328–331

Willbold M, Elliott T, Moorbath S (2011) The tungsten isotopic composition of the Earth's mantle before the terminal bombardment. Nature 477:195–198

Willbold M, Mojzsis SJ, Chen H-W, Elliott T (2015) Tungsten isotope composition of the Acasta Gneiss Complex. Earth Planet Sci Lett 419:168–177

Wood BJ, Halliday AN (2005) Cooling of the Earth and core formation after the giant impact. Nature 437:1345–1348